



HAL
open science

EuxSr_{1-x}C₂ ($0 \leq x \leq 1$): A Dicarbide Solid Solution with Perfect Vegard Behavior

Uwe Ruschewitz, Pascal Link, Derk Wandner, Inga Schellenberg, Rainer Pöttgen, Michael Paulus, Christoph Sahle, Christian Sternemann

► **To cite this version:**

Uwe Ruschewitz, Pascal Link, Derk Wandner, Inga Schellenberg, Rainer Pöttgen, et al.. EuxSr_{1-x}C₂ ($0 \leq x \leq 1$): A Dicarbide Solid Solution with Perfect Vegard Behavior. *Journal of Inorganic and General Chemistry / Zeitschrift für anorganische und allgemeine Chemie*, 2010, 636 (12), pp.2276. 10.1002/zaac.201000206 . hal-00583554

HAL Id: hal-00583554

<https://hal.science/hal-00583554v1>

Submitted on 6 Apr 2011

HAL is a multi-disciplinary open access archive for the deposit and dissemination of scientific research documents, whether they are published or not. The documents may come from teaching and research institutions in France or abroad, or from public or private research centers.

L'archive ouverte pluridisciplinaire **HAL**, est destinée au dépôt et à la diffusion de documents scientifiques de niveau recherche, publiés ou non, émanant des établissements d'enseignement et de recherche français ou étrangers, des laboratoires publics ou privés.



**EuxSr_{1-x}C₂ (0 ≤ x ≤ 1): A Dicarbide Solid Solution with
Perfect Vegard Behavior**

Journal:	<i>Zeitschrift für Anorganische und Allgemeine Chemie</i>
Manuscript ID:	zaac.201000206.R1
Wiley - Manuscript type:	Article
Date Submitted by the Author:	08-Jul-2010
Complete List of Authors:	Ruschewitz, Uwe; Universitaet zu Koeln, Department fuer Chemie Link, Pascal Wandner, Derk Schellenberg, Inga Pöttgen, Rainer Paulus, Michael Sahle, Christoph Sternemann, Christian
Keywords:	Dicarbide, Solid solution, Europium, Synchrotron powder diffraction, Mössbauer spectroscopy



ARTICLE

DOI: 10.1002/zaac.200((will be filled in by the editorial staff))

Eu_xSr_{1-x}C₂ (0 ≤ x ≤ 1): A Dicarbide Solid Solution¹ with Perfect Vegard Behavior**Pascal Link^[a], Derk Wandner^[a], Inga Schellenberg^[b], Rainer Pöttgen^[b], Michael Paulus^[c],
Christoph J. Sahle^[c], Christian Sternemann^[c], and Uwe Ruschewitz^{*[a]}***Contribution from the SPP 1166 “Lanthanide Specific Functionalities in Molecules and Materials”***Keywords:** Dicarbides; Solid Solution; Europium; Valence State; Synchrotron Powder Diffraction; Mössbauer Spectroscopy

A solid solution Eu_xSr_{1-x}C₂ (0 ≤ x ≤ 1) was synthesized by direct reaction of the elements at 1123 K. The crystal structures of these compounds, investigated by synchrotron powder diffraction, depend upon x. For x > 0.5 the monoclinic ThC₂ type structure (C2/c, Z = 4) is observed and for x ≤ 0.5 the ThC₂ type structure coexists with the tetragonal CaC₂ type structure (I4/mmm, Z = 2). The unit cell volumes per formula unit of all Eu_xSr_{1-x}C₂ compounds show perfect Vegard behaviour, which is due to the almost identical ionic radii of Eu²⁺ and Sr²⁺. Mössbauer spectroscopic investigations indeed reveal that Eu is in the divalent state over the whole composition range. Eu_xSr_{1-x}C₂ exhibits several temperature

dependent phase transitions that were studied by synchrotron powder diffraction and differential thermal analysis. The transition to a cubic high-temperature modification (*Fm* $\bar{3}$ m, Z = 4) is of special interest, as it contains information about strain effects appearing inside the modifications with ordered C₂ dumbbells (ThC₂ and CaC₂ type structures). The linear temperature dependence of the obtained transition temperatures T_{ph} shows that no observable strain exists in Eu_xSr_{1-x}C₂, which is again due to the almost identical radii of Eu²⁺ and Sr²⁺. Eu_xSr_{1-x}C₂ may therefore be described as a strain free dicarbide solid solution with perfect Vegard behaviour.

¹ According to the classical definition Eu_xSr_{1-x}C₂ is not a solid solution, as SrC₂ (I4/mmm, Z = 2) and EuC₂ (C2/c, Z = 4) are not isotopic. In a correct description two solid solutions – Eu dissolved in SrC₂ and Sr dissolved in EuC₂ – are formed. But as a Vegard behavior is found for the complete series Eu_xSr_{1-x}C₂ the term “solid solution” will be used for it throughout the manuscript. This is in agreement with the common use of this term in large parts of the respective literature.

- [a] Department of Chemistry, University of Cologne,
GreinstraÙe 6, D-50939 Kln (Germany)
Fax: +49-(0)-221-470-3933
E-mail: Uwe.Ruschewitz@uni-koeln.de
- [b] Institute of Inorganic and Analytical Chemistry, WWU
Mnster, CorrensstraÙe 30, D-48149 Mnster (Germany)
- [c] Fakultt Physik / DELTA, Technische Universitt Dortmund,
Maria-Goeppert-Mayer-StraÙe 2, D-44221 Dortmund
(Germany)

Introduction

Dicarbides of rare earth (RE_2 , RE = rare earth metal) and alkaline earth metals (AEC_2 , AE = alkaline earth metal) have been known for a long time. Although they exhibit identical crystal structures, their physical properties are completely different, i.e. metallic (REC_2) vs. insulating behavior (AEC_2). In a simple picture this can be attributed to an additional electron in REC_2 according to $\text{RE}^{3+}(\text{C}_2^{2-})(e^-)$. This additional electron is delocalized in a conduction band. Only very recently we showed that the dicarbide of Europium (EuC_2) shows semiconducting behavior [1]. At ambient conditions it crystallizes – differing to all other REC_2 , which are known to exist in the CaC_2 type structure ($I4/mmm$, $Z = 2$) – in the ThC_2 type structure ($C2/c$, $Z = 4$). These observations reveal that EuC_2 resembles more the AEC_2 than the REC_2 compounds. Accordingly, measurements of the Mssbauer effect show that Eu is clearly in a divalent state in EuC_2 [1].

Solid solutions of rare earth metal dicarbides $\text{RE}'_x\text{RE}''_{1-x}\text{C}_2$ have been known since the seventies [2, 3]. However, dicarbides of composition $\text{RE}_x\text{AE}_{1-x}\text{C}_2$ have been reported only for the system $\text{CaC}_2\text{-YbC}_2$ [4]. The formation of solid solutions often leads to dramatic changes in the properties of the respective compounds. Electrical resistivity or magnetism may be changed drastically by mixed occupation of metal sites as well as the stability range of different polymorphs. Solid solutions $\text{RE}_x\text{AE}_{1-x}\text{C}_2$ seem to be especially interesting in this context, as the binary compounds REC_2 and AEC_2 may differ strongly in their physical properties (s. above). Therefore, we have started to investigate the synthesis of $\text{RE}_x\text{AE}_{1-x}\text{C}_2$ solid solutions as well as the characterization of their structural and physical properties. In a first attempt we have chosen the system $\text{Eu}_x\text{Sr}_{1-x}\text{C}_2$, as Eu^{2+} (135 pm [5], CN = 10) and Sr^{2+} (136 pm [5], CN = 10) have very similar ionic radii. With these requirements the formation of a strain free solid solution with perfect Vegard behavior was expected.

Results and Discussion

We were able to synthesize a solid solution series $\text{Eu}_x\text{Sr}_{1-x}\text{C}_2$ with $0 \leq x \leq 1$. The successful synthesis of 12 compounds with differing x was clearly proven by synchrotron powder diffraction data. All compounds – with the exception of SrC_2 , which is colorless – are black, microcrystalline powders that show a high sensitivity to oxygen and moisture. The gases released during this decomposition have not been analyzed up to now, but our preliminary Mssbauer investigations on EuC_2 with a not completely air-tight sample holder indicated that the final product of this decomposition contains Eu^{3+} . Due to strong X-ray absorption of Eu, diffractometers with conventional $\text{CuK}_{\alpha 1}$ radiation are not suitable; moreover $\text{MoK}_{\alpha 1}$ radiation

provides powder diffractograms with only a very poor angular resolution. Therefore, synchrotron radiation using a short wavelength is the appropriate tool to obtain powder data with good resolution and minimized absorption.

The resulting patterns were first indexed and subsequently refined by the Rietveld method to get reliable cell parameters and phase ratios. The known crystal structures of EuC_2 [1] and SrC_2 [6] were used as starting models for the refinement. Figure 1 shows the Rietveld refinement of $\text{Eu}_{0.5}\text{Sr}_{0.5}\text{C}_2$ as an example for the quality of the data and the refinement. All samples appeared homogeneous and no reflections for any impurity phases were observed. Neither a splitting of reflections nor unusual broad reflections were observed so that the existence of two phases, i.e. SrC_2 and EuC_2 in varying ratios can be excluded.

In all final refinements the composition x – i.e. the occupancy of the mixed metal sites with Eu and Sr, resp. – has not been refined, as it led to physical meaningless results in most cases. Instead the composition x was taken from the ratio of the starting materials Eu and Sr. The inaccuracy of weighing was taken into account by applying an error of ± 0.03 to all compositions (see Figure 2). Neutron diffraction experiments on similar solid solutions with Ytterbium (unpublished) confirm the validity of this assumption. Furthermore, atomic positions and displacement parameters of C were not refined, as the scattering power of C is too low compared with Eu or Sr to obtain reliable results. Instead the atomic positions of C in EuC_2 [1] and SrC_2 [6] were used and U_{iso} was fixed to 400 pm^2 . Details of the refinement of $\text{Eu}_{0.5}\text{Sr}_{0.5}\text{C}_2$, representative for all other compounds, are presented in Table 1.

Table 1. $\text{Eu}_{0.5}\text{Sr}_{0.5}\text{C}_2$: Summary of Rietveld refinement (295 K, synchrotron powder diffraction data, $\lambda = 65.255 \text{ pm}$, Beamline BL9 at DELTA / Dortmund).

	ThC_2 type structure	CaC_2 type structure
Space group, Z	$C2/c$ (no. 15), 4	$I4/mmm$ (no. 139), 2
a / pm	703.13(4)	411.68(9)
b / pm	442.74(3)	
c / pm	761.29(4)	671.1(3)
$\beta / ^\circ$	107.122(5)	
V / nm^3	0.22649(2)	0.11374(5)
Eu / Sr ^[a]	4 e, $y = 0.1828(4)$	2 a
$U_{\text{iso}} / \text{pm}^2$	100(10)	100 ^[b]
C	not refined (s. text)	not refined (s. text)
No. of reflections	93	22
R_{Bragg}	0.0360	0.0396
Mass fraction / %	94.05(4)	5.9(2)
R_p		0.0132
wR_p		0.0195
No. of refined parameters		30

^[a] U_{iso} and atomic positions of metal ions have been constrained.

^[b] U_{iso} fixed due to small fraction of the phase

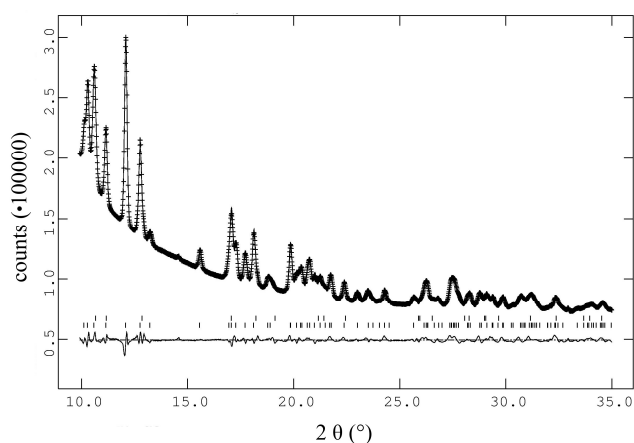


Figure 1. Rietveld refinement of $\text{Eu}_{0.5}\text{Sr}_{0.5}\text{C}_2$ (295 K, $\lambda = 65.255$ pm, BL9 / DELTA) showing the observed (+) and calculated patterns (solid line) as well as the difference between them. Vertical bars mark the positions of the reflections of CaC_2 type structure ($I4/mmm$, $Z = 2$; upper bars) and ThC_2 type structure ($C2/c$, $Z = 4$; lower bars).

All compounds show crystal structures that are known for the AEC_2 series (AE = Ca [7], Sr [6], Ba [8]). As can be seen in Figure 2, the structure formed at room temperature (RT) depends on the composition x . For $x > 0.5$ only the monoclinic ThC_2 type structure ($C2/c$, $Z = 4$) is found, which is the stable modification of EuC_2 at RT [1]. For $x \leq 0.5$ the ThC_2 type structure coexists with the tetragonal CaC_2 type structure ($I4/mmm$, $Z = 2$), the stable modification of SrC_2 at RT [6]. The relative amount of the tetragonal modification decreases with x . All refined volumes per formula unit are in good agreement with Vegard's law, no strong deviations occur (see Figure 3). These findings already suggest that Eu is divalent over the whole composition range, as a change of the Eu valence to + III should lead to a significant reduction of the unit cell volume. In Figure 3 it can be seen that for $0.1 \leq x \leq 0.5$ both modifications coexist. For $x < 0.33$ the CaC_2 type structure shows the higher density, whereas for $x > 0.33$ the density of the ThC_2 type structure is higher. For $x = 0.33$ the density of both modifications is almost the same. This is roughly coinciding with the appearance as a major component in this system: below $x \approx 0.2$ the CaC_2 type structure dominates, above $x \approx 0.2$ the ThC_2 type structure (Figure 2). Thus, this behavior seems to be mainly governed by thermodynamics. But as both phases coexist, there are probably also kinetic effects that control the equilibrium composition as well as its change with increasing temperature.

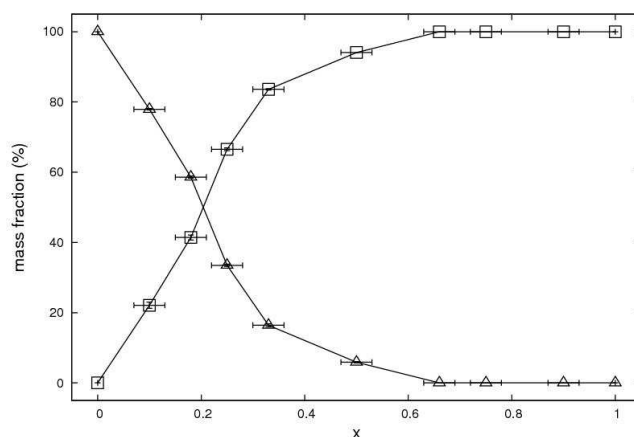


Figure 2. Mass fraction of the different modifications of $\text{Eu}_x\text{Sr}_{1-x}\text{C}_2$ as a function of x at RT. Open squares (\square) show the ThC_2 type structure, open triangles (Δ) the CaC_2 type structure.

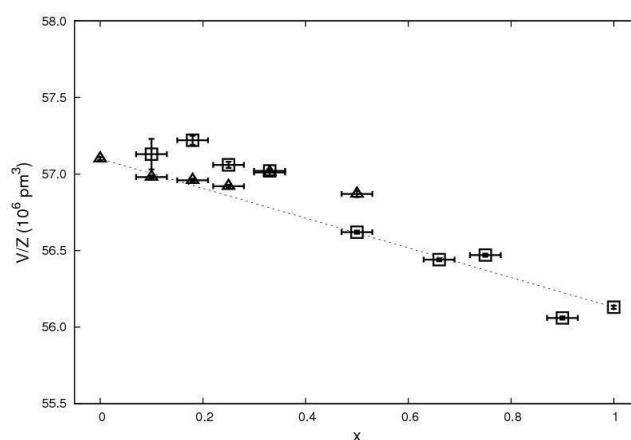


Figure 3. Unit cell volume per formula unit of the different modifications of $\text{Eu}_x\text{Sr}_{1-x}\text{C}_2$ as a function of x . Open squares (\square) show the ThC_2 type structure, open triangles (Δ) the CaC_2 type structure. A behavior according to Vegard's law is indicated by a dotted straight line. Errors bars for the weighing and the volume errors are given. The latter are in most cases smaller than the symbol used in the figure.

To verify the existence of Eu^{2+} in $\text{Eu}_x\text{Sr}_{1-x}\text{C}_2$ ^{151}Eu Mössbauer spectra of five selected compounds with $x = 0.1, 0.25, 0.5, 0.75,$ and 0.9 were recorded at 77 K (Figure 4). Low temperatures were chosen to obtain spectra of improved quality. Unfortunately, we do not know, whether $\text{Eu}_x\text{Sr}_{1-x}\text{C}_2$ compounds undergo phase transitions at low temperatures. This is part of our current work. But the very good agreement with the Mössbauer parameters obtained for pure EuC_2 (see below) confirm our assumption that Eu is present as Eu^{2+} in $\text{Eu}_x\text{Sr}_{1-x}\text{C}_2$.

The corresponding fitting parameters of the Mössbauer measurements on $\text{Eu}_x\text{Sr}_{1-x}\text{C}_2$ are listed in Table 2. All spectra could be well reproduced with single signals subject to quadrupole splitting due to the non-cubic site symmetry. The isomer shift as well as the quadrupole interaction are comparable to EuC_2 ($\delta = -11.92(3)$ mm/s, $\Delta E_Q = 4.3(3)$ mm/s) [1]. There is no trend in the δ , ΔE_Q , and Γ values over the whole x range, indicating that the local electronic situation around the europium atoms is quite similar.

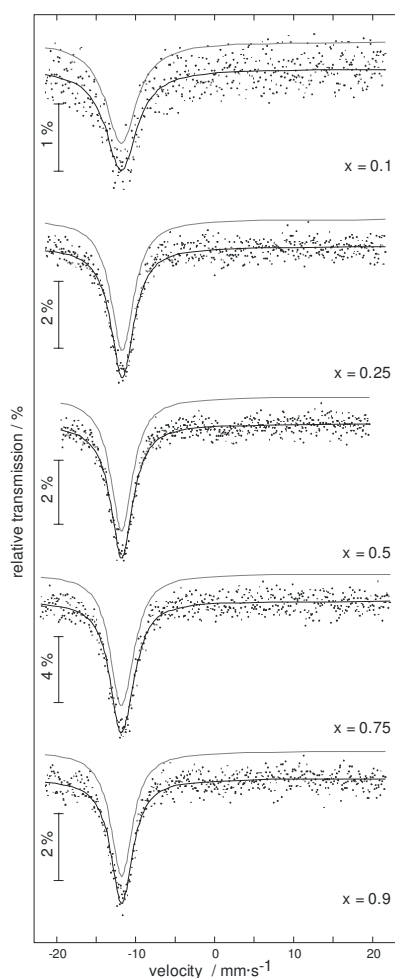


Figure 4. Experimental and simulated ^{151}Eu Mössbauer spectra of the $\text{Eu}_x\text{Sr}_{1-x}\text{C}_2$ samples with $x = 0.1, 0.25, 0.5, 0.75,$ and 0.9 (77 K data).

Table 2. Fitting parameters of ^{151}Eu Mössbauer spectroscopic measurements (77 K data) of $\text{Eu}_x\text{Sr}_{1-x}\text{C}_2$. Numbers in parentheses represent the statistical errors in the last digit. (δ), isomer shift; (Γ), experimental line width; (ΔE_Q), electric quadrupole splitting parameter. * fixed parameter.

Compound	x	$\delta / \text{mm}\cdot\text{s}^{-1}$	$\Gamma / \text{mm}\cdot\text{s}^{-1}$	$\Delta E_Q / \text{mm}\cdot\text{s}^{-1}$
$\text{Eu}_x\text{Sr}_{1-x}\text{C}_2$	0.1	-11.95(7)	2.70*	4.5*
	0.25	-11.86(4)	2.6(1)	4.4(4)
	0.5	-11.91(3)	2.7(1)	3.7(3)
	0.75	-11.87(4)	2.7(1)	4.3(4)
	0.9	-11.91(4)	2.4(1)	4.2(3)

As EuC_2 and SrC_2 are known to show temperature dependent phase transformations [1, 6], the structural behavior of four selected compounds $\text{Eu}_x\text{Sr}_{1-x}\text{C}_2$ with $x = 0.18, 0.25, 0.5,$ and 0.75 was studied in the temperature range 300–800 K using synchrotron powder diffraction. All compounds show a continuous transformation from the ThC_2 type structure to the CaC_2 type structure with increasing temperature so that both structures coexist over a broad temperature range. Only for $x = 0.18$ a complete transformation can be observed: above 580 K the CaC_2 type structure is the only detectable phase. At temperatures between 600 and 700 K all compounds show a sharp transformation to a cubic high temperature modification ($Fm\bar{3}m$, $Z = 4$), which is also known for both binary carbides [1, 6]. From synchrotron powder diffraction no

exact transition temperatures T_{Ph} could be determined due to the large applied temperature steps of 50 K. Representative powder patterns as well as mass fractions of the observable modifications at different temperatures are presented in Figures 5 and 6.

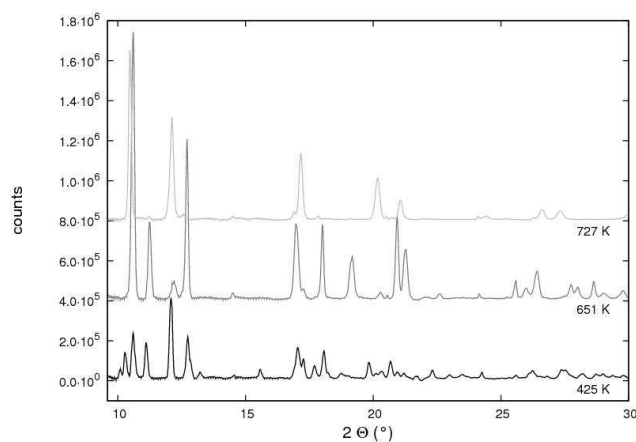


Figure 5. Synchrotron powder patterns (background corrected) of $\text{Eu}_{0.5}\text{Sr}_{0.5}\text{C}_2$ at different temperatures. The pattern obtained at 425 K mainly shows the ThC_2 type structure, whereas at 651 K mainly the CaC_2 type structure and at 727 K the cubic high temperature modification are observed.

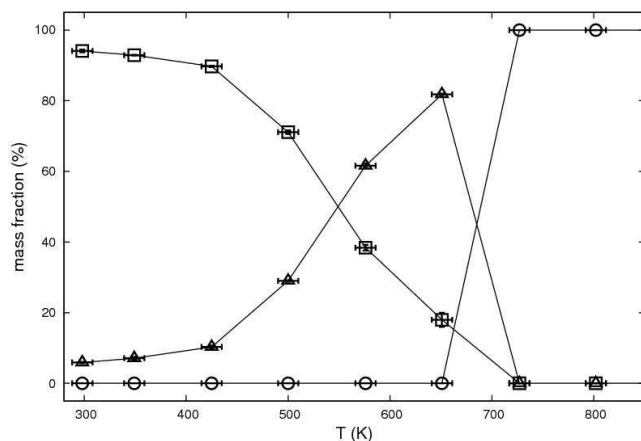


Figure 6. Mass fraction of the different modifications of $\text{Eu}_{0.5}\text{Sr}_{0.5}\text{C}_2$ as a function of temperature. Open squares (\square) show the ThC_2 type structure, open triangles (Δ) the CaC_2 type structure and open circles (\circ) the cubic high temperature modification.

To determine the transition temperatures T_{Ph} more accurately, the thermal behavior of the compounds was analyzed by differential thermal analysis (DTA). The high temperature phase transition that can be regarded as an order-disorder transformation shows a significant uptake of heat that can be observed as an endothermic peak in the DTA. In contrast, the transition between the ThC_2 and CaC_2 type structures, a displacive transformation in the second coordination sphere, does not show an observable evolution of heat. It is therefore not detectable in the DTA. It is remarkable that the high temperature phase transition peaks of $\text{Eu}_x\text{Sr}_{1-x}\text{C}_2$ are much broader than the peaks of the pure dicarbides. The halfwidth increases from $x = 0$ to 0.5 and decreases again from $x = 0.5$ to 1, which implies that this effect arises from the mixed occupancy of the metal site. As

a consequence, the transition temperatures (T_{Ph}) could not be determined by fitting a Gaussian to the peaks. Instead, the temperatures were taken from the measured curves by inspection with errors estimated from the broadness of the respective peaks. The results can be seen in Table 3 and Figure 7.

Table 3. Transition temperatures T_{Ph} of $\text{Eu}_x\text{Sr}_{1-x}\text{C}_2$ with estimated errors obtained from DTA measurements.

x	T_{Ph} / K
0	698 ± 2
0.1	687 ± 5
0.18	685 ± 8
0.25	680 ± 10
0.33	674 ± 10
0.5	662 ± 10
0.66	650 ± 10
0.75	635 ± 8
0.9	633 ± 5
1	631 ± 2

All temperatures T_{Ph} range from 600 to 700 K, which shows a good agreement between powder diffraction and DTA results. Within the limits of accuracy, all T_{Ph} values lie on a straight line between the pure dicarbides. This finding may be interpreted by using the Lattice Strain Theory of *McColm et al.* [2, 3], who carried out similar studies on $\text{RE}_x\text{RE}'_{1-x}\text{C}_2$ solid solutions. Within this theory the mixed occupancy of the metal site causes a lattice strain inside the modifications with ordered C_2 dumbbells (ThC_2 and CaC_2 type structures), if the metal ions differ in their ionic radii. The strain should be proportional to the difference in the ionic radii as well as to the amount of mixing, with a theoretical maximum at $x = 0.5$. This strain energy causes an increase of the enthalpy H of the ordered phase, which results in a decrease of ΔH_{Ph} and T_{Ph} . Therefore the transition temperatures T_{Ph} of $\text{RE}_x\text{RE}'_{1-x}\text{C}_2$ solid solutions do not show a straight line between $x = 0$ and $x = 1$, but exhibit a characteristic minimum, whose value depends on the difference in the cations' radii.

The linear behavior of T_{Ph} observed for $\text{Eu}_x\text{Sr}_{1-x}\text{C}_2$ can be also explained by using *McColm's* strain theory. As the divalent ions Eu^{2+} and Sr^{2+} do not show a noticeable difference in their ionic radii, no strain should arise in the ordered phases from the mixed occupancy of the metal site. As a consequence, T_{Ph} does not show a local minimum in this solid solution. Thus, the values of T_{Ph} can simply be calculated by the linear relationship $T_{\text{Ph}}(\text{Eu}_x\text{Sr}_{1-x}\text{C}_2) = x \cdot T_{\text{Ph}}(\text{EuC}_2) + (1-x) \cdot T_{\text{Ph}}(\text{SrC}_2)$, analogous to the respective volumes.

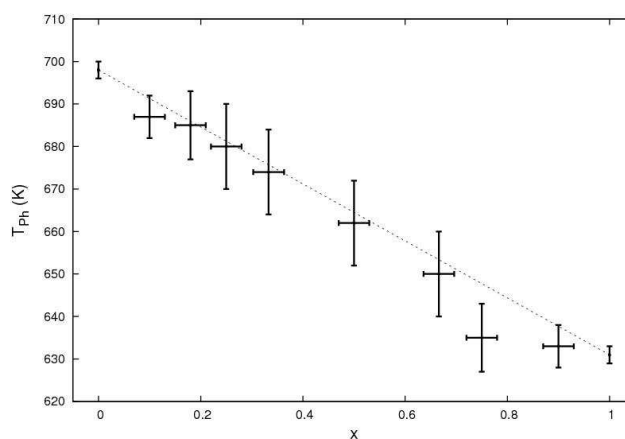


Figure 7. Transition temperatures T_{Ph} of $\text{Eu}_x\text{Sr}_{1-x}\text{C}_2$ as a function of x . All values were obtained from DTA measurements. The dotted straight line indicates a hypothetical strain free system (see text).

Conclusions

Our investigations show that the solid solution $\text{Eu}_x\text{Sr}_{1-x}\text{C}_2$ can be prepared without impurity phases by direct reaction of the elements at 1123 K. The system shows miscibility in the whole composition range ($0 \leq x \leq 1$). All samples – with the exception of colourless SrC_2 – are black microcrystalline powders.

The used analytical methods show that the compounds $\text{Eu}_x\text{Sr}_{1-x}\text{C}_2$ can be described as a solid solution with a perfect Vegard behaviour comprising Eu^{2+} ions. Synchrotron powder diffraction experiments reveal that $\text{Eu}_x\text{Sr}_{1-x}\text{C}_2$ crystallizes in the well-known ThC_2 and CaC_2 type structures at RT, the type of structure depends on x . The unit cell volumes per formula unit of all compounds satisfy Vegard's law, as they lie on a straight line between the pure dicarbides EuC_2 and SrC_2 . Moreover, measurements of the Mössbauer effect proved Eu^{2+} for all $\text{Eu}_x\text{Sr}_{1-x}\text{C}_2$ compounds investigated, as was also found for pure EuC_2 [1]. All compounds transform to a cubic high temperature modification that is well-known for both REC_2 and AEC_2 . Both temperature dependent synchrotron powder diffraction and DTA measurements revealed that the high temperature phase transition temperatures T_{Ph} of all compounds lie on a straight line between the pure dicarbides. This observation is due to the nearly identical ionic radii of Eu^{2+} and Sr^{2+} and can be interpreted using the strain theory of *McColm et al.* [2, 3].

The successful synthesis of $\text{Eu}_x\text{Sr}_{1-x}\text{C}_2$ is not very surprising, as Eu^{2+} and Sr^{2+} have very similar ionic radii. But in the meantime, we were able to synthesize solid solutions containing metal ions with more differing radii, e.g. $\text{Yb}_x\text{Ca}_{1-x}\text{C}_2$. Here, an interesting valence change of Yb from +2 to +3 was observed, depending upon x . This will be part of an upcoming contribution.

Experimental Section

Synthesis. All $\text{Eu}_x\text{Sr}_{1-x}\text{C}_2$ compounds were prepared by direct reaction of the elements inside a tantalum bomb containing an inert atmosphere. Eu metal (Chempur, 99.99 %) and Sr metal (Sigma Aldrich, 99.99 %) were filed to fine powders and mixed with

graphite powder (Sigma Aldrich, 99.9998 %) in the desired molar ratio. Prior to the reaction the graphite powder was heated at 1073 K in a dynamic vacuum for 48 hours to remove water and oxygen inclusions. In a typical reaction 114.0 mg Eu (0.75 mmol), 65.7 mg Sr (0.75 mmol) and 39.6 mg graphite (3.3 mmol) were thoroughly mixed in a glove box (argon atmosphere) and were afterwards transferred to a tantalum ampoule. A small excess of graphite was used to suppress the formation of oxides and consider losses of graphite during the transfer process. The tantalum ampoules were then sealed using an arc furnace with a helium atmosphere of 750 mbar pressure. A current of 10 A was used to melt the tantalum metal. Subsequently the ampoules were encapsulated in silica glass tubes under vacuum to avoid an oxidation of the tantalum at high temperatures. The resulting ampoules were then transferred to a tube furnace and heated to 1123 K within 4 hours. The reaction was maintained at this temperature for 24 hours, afterwards the furnace was cooled down to room temperature within 8 hours. All sample handling was carried out in a glovebox in an argon atmosphere. Sample purity was checked by X-ray powder diffraction (Huber G670, MoK α_1 radiation, glass capillary \varnothing 0.3 mm).

Synchrotron powder diffraction. Synchrotron powder patterns were recorded at beamline BL9 [9] of the DELTA synchrotron (University of Dortmund, Germany). All measurements were carried out in glass or silica glass capillaries (\varnothing 0.3 mm) that were loaded in a glove box (argon atmosphere). For high temperature measurements a furnace was used, which allowed measurements up to 900 K. A photon energy of 19 keV ($\lambda = 65.255$ pm) was chosen to minimize sample absorption. For fast data collection a MAR345 area detector was used. The obtained powder rings were subsequently integrated by using the program FIT2D [10] to receive one-dimensional powder patterns.

All Rietveld refinements were carried out with the GSAS suite of programs [11].

Mössbauer spectroscopy. The 21.53 keV transition of ^{151}Eu with an activity of 130 MBq (2 % of the total activity of a $^{151}\text{Sm}:\text{EuF}_3$ source) was used for the ^{151}Eu Mössbauer spectroscopic experiments. The measurements were performed in the usual transmission geometry at 77 K. The source was kept at room temperature in all experiments. The samples were placed within thin-walled sealed glass containers at a thickness corresponding to about 10 mg Eu/cm 2 . Fitting of the spectra was performed with the NORMOS-90 program system [12].

Differential thermal analysis. DTA measurements were carried out using a Netzsch STA 409 Cell thermobalance placed in a glove box (nitrogen atmosphere). Approximately 20 mg of the sample were weighed into an aluminum oxide crucible and subsequently heated to 873 K in an argon stream with a heating rate of 10 K/min. An empty aluminum oxide crucible was heated simultaneously as reference material. Afterwards the furnace was cooled down to room temperature with a cooling rate of 10 K/min. The temperature difference between sample and reference was detected by using Pt-Rh/Pt thermocouples.

Acknowledgments

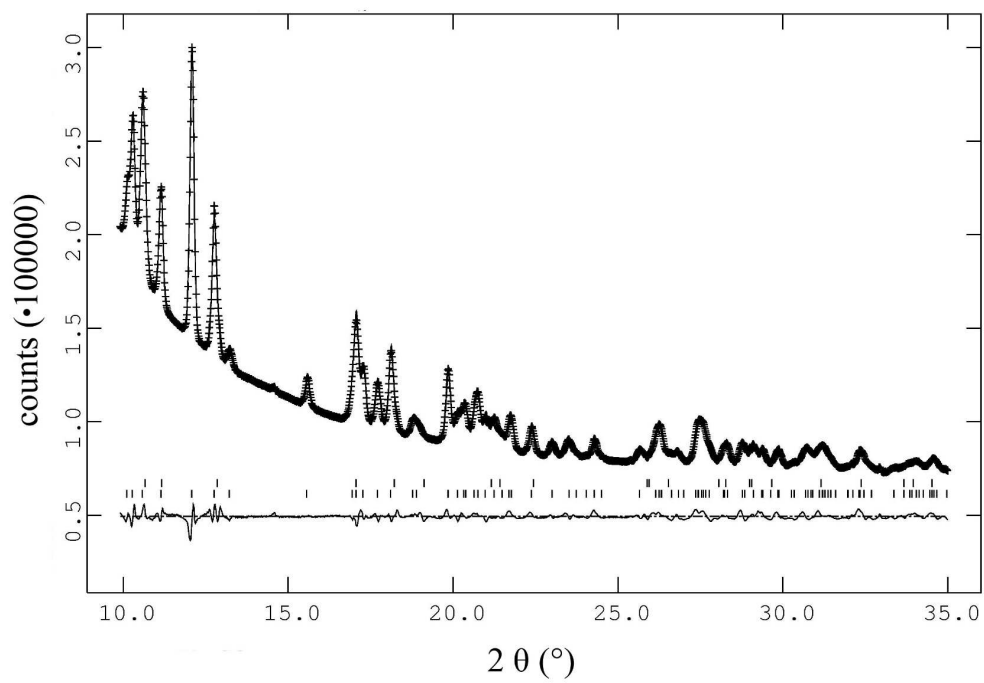
This work was financially supported by the Deutsche Forschungsgemeinschaft through SPP 1166 *Lanthanoidspezifische Funktionalitäten in Molekül und Material*. The authors acknowledge DELTA for providing synchrotron radiation.

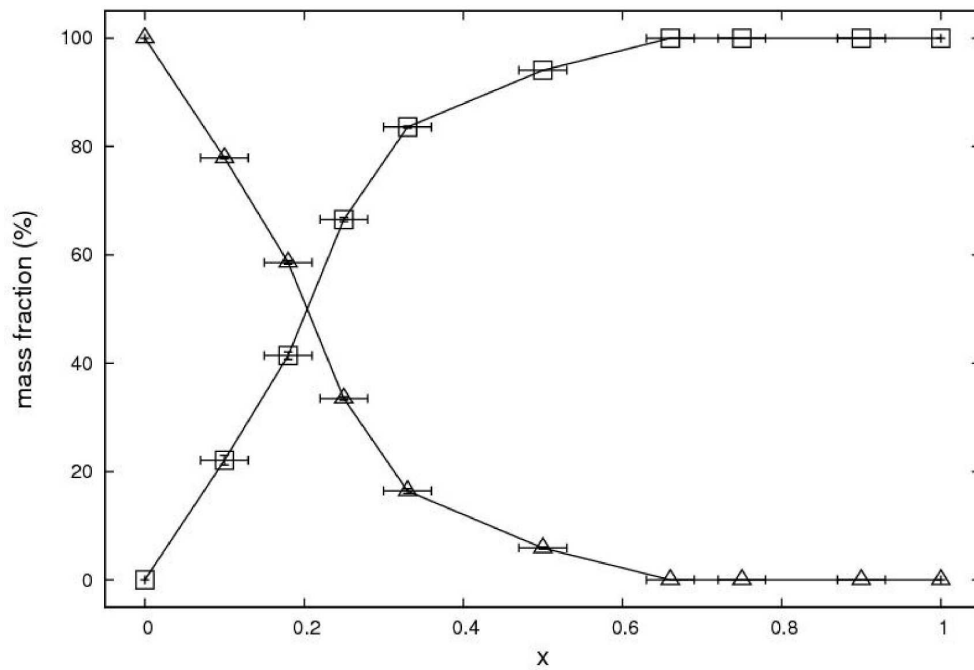
- [1] D. Wandner, P. Link, O. Heyer, J. Mydosh, M. A. Ahmida, M. M. Abd-Elmeguid, M. Speldrich, H. Lueken, U. Ruschewitz, *Inorg. Chem.* **2010**, *49*, 312.
- [2] I. J. McColm, N. J. Clark, I. Colquhoun, *J. Inorg. Nucl. Chem.* **1972**, *34*, 3809.
- [3] I. J. McColm, N. J. Clark, T. A. Quigley, *J. Inorg. Nucl. Chem.* **1973**, *35*, 1931.
- [4] B. Hájek, V. Brožek, M. Popl, *Collect. Czech. Chem. Commun.* **1971**, *36*, 1537.
- [5] D. R. Lide, *CRC Handbook of Chemistry and Physics*. **2000**, 81st Edition, 12-14.
- [6] V. Vohn, M. Knapp, U. Ruschewitz, *J. Solid State Chem.* **2000**, *151*, 111.
- [7] M. Knapp, U. Ruschewitz, *Chem. Eur. J.* **2001**, *7*, 874.
- [8] V. Vohn, W. Kockelmann, U. Ruschewitz, *J. Alloys Compd.* **1999**, *284*, 132.
- [9] C. Krywka, M. Paulus, C. Sternemann, M. Volmer, A. Remhof, G. Nowak, A. Nefedov, B. Pöter, M. Spiegel, M. Tolan, *J. Synchrotron Rad.* **2006**, *13*, 8.
- [10] J. Hammersley, *Fit2d user manual*. **1996**, ESRF.
- [11] A. C. Larson, R. B. v. Dreele, *Los Alamos Laboratory, Rep. No. LA-UR* **1987**, *86*, 748.
- [12] R. A. Brand, *Normos Mössbauer fitting Program* (Universität Duisburg) **2002**.

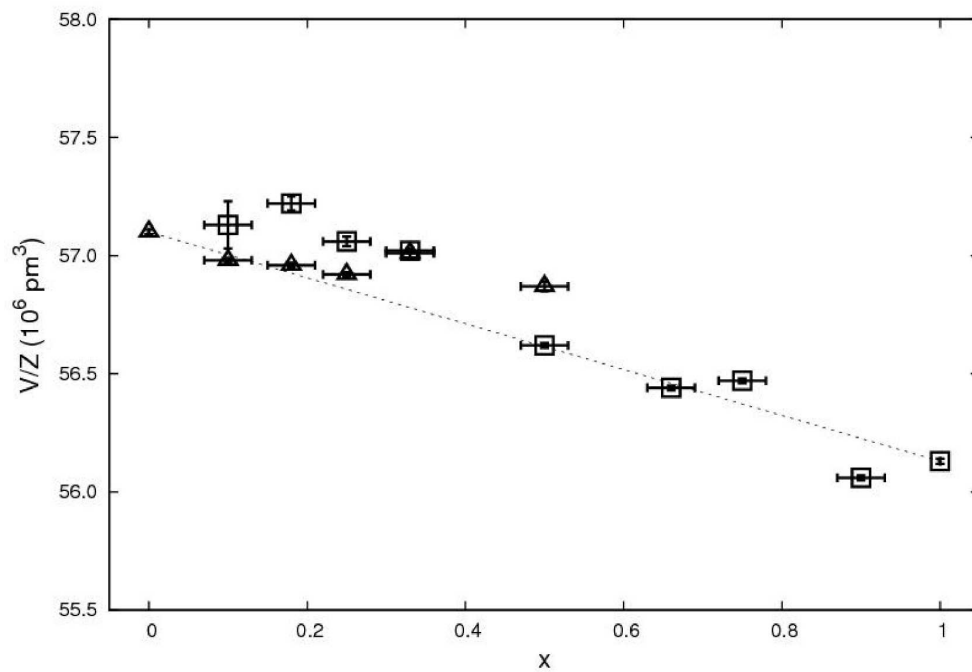
Received: ((will be filled in by the editorial staff))

Published online: ((will be filled in by the editorial staff))

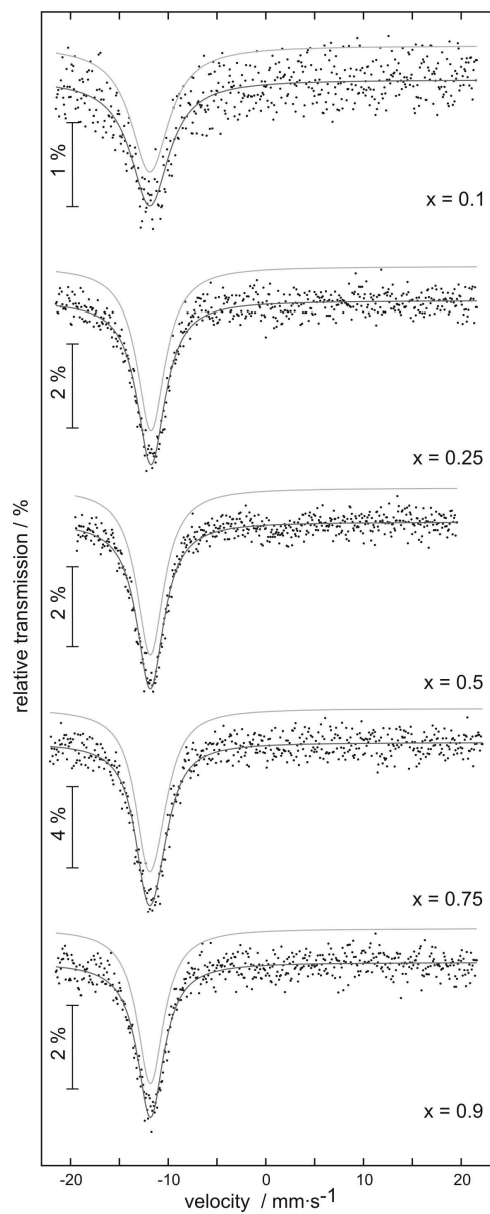
1
2
3
4
5
6
7
8
9
10
11
12
13
14
15
16
17
18
19
20
21
22
23
24
25
26
27
28
29
30
31
32
33
34
35
36
37
38
39
40
41
42
43
44
45
46
47
48
49
50
51
52
53
54
55
56
57
58
59
60

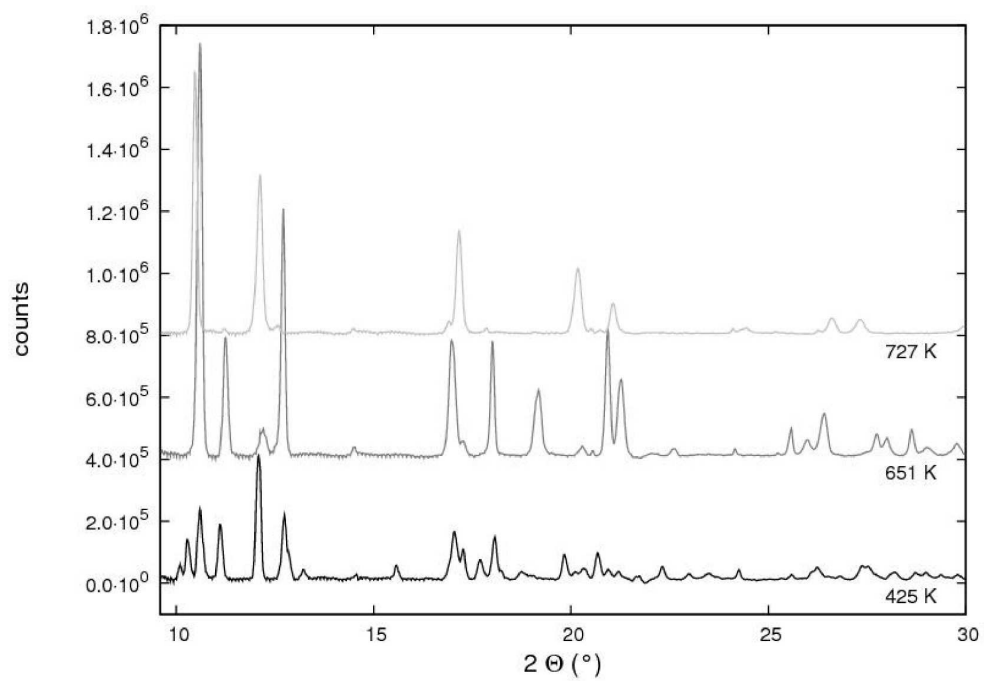


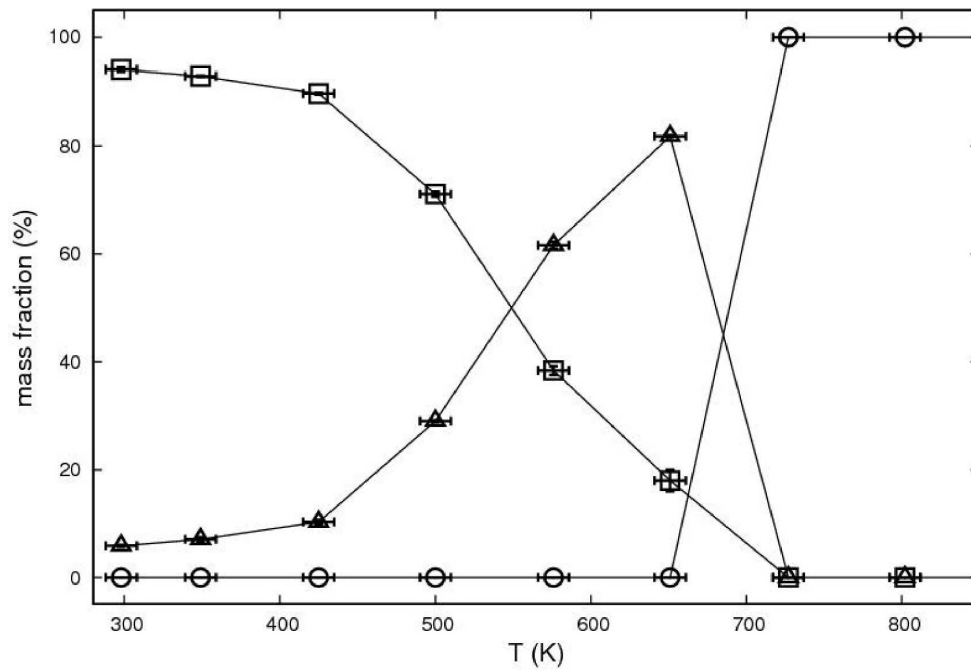




1
2
3
4
5
6
7
8
9
10
11
12
13
14
15
16
17
18
19
20
21
22
23
24
25
26
27
28
29
30
31
32
33
34
35
36
37
38
39
40
41
42
43
44
45
46
47
48
49
50
51
52
53
54
55
56
57
58
59
60







1
2
3
4
5
6
7
8
9
10
11
12
13
14
15
16
17
18
19
20
21
22
23
24
25
26
27
28
29
30
31
32
33
34
35
36
37
38
39
40
41
42
43
44
45
46
47
48
49
50
51
52
53
54
55
56
57
58
59
60

